

Determination of the chromospheric quiet network element area index and its variation between 2008 and 2011

Jagdev Singh, Ravindra Belur, Selvendran Raju, Kumaravel Pichaimani, Muthu Priyal, Thambaje Gopalan Priya and Amareswari Kotikalapudi

Indian Institute of Astrophysics, Koramangala, Bengaluru-560 034, India; jsingh@iiap.res.in

Received 2011 August 12; accepted 2011 October 8

Abstract In general, it is believed that plages and sunspots are the main contributors to solar irradiance. There are small-scale structures on the Sun with intermediate magnetic fields that could also contribute to solar irradiance, but it has not yet been quantified how many of these small scale structures contribute and how much this varies over the solar cycle. We used Ca II K images obtained from the telescope at the Kodaikanal observatory. We report a method to separate the network elements from the background structure and plage regions, and compute the changes in the network element area index during the minimum phase of the solar cycle and part of the ascending phase of cycle 24. The measured area occupied by the network elements is about 30% and the plages cover less than 1% of the solar disk during the observation period from February 2008 to 2011. During the extended period of minimum activity, it is observed that the network element area index decreases by about 7% compared to the area occupied by the network elements in 2008. A long term study of the network element area index is required to understand the variations over the solar cycle.

Key words: Sun: network — Sun: Ca-K — Sun: solar cycle

1 INTRODUCTION

Synoptic observations of the Sun are very important in studying the long term variations of the solar magnetic field and its effect on space weather and climate. The large- and small-scale structures observed on the Sun contribute to the solar irradiances in different magnitudes at different times of the solar cycle (Worden et al. 1998). The small-scale network structures can be observed at the chromospheric level and above in the solar atmosphere. The contrast between the network structures is large in the Ca II K wavelength band. The main features we observe in the line center of the Ca-K images are the plages, the active network, the enhanced network and network regions. Many have used the Ca-K images to estimate the contribution of the plages and the network to the total solar irradiance at different times of the epoch (Worden et al. 1998). Several authors have used different techniques to compute the Ca-K plage index using the data from the Kodaikanal, Mt. Wilson, Arcetri and Sac Peak observatories and compared the results obtained from different data sets (Foukal et al. 2009; Tlatov et al. 2009; Ermolli et al. 2009).

Many techniques have been developed to estimate the area of the network, and the data describing most of these results are restricted to a small time period. Hagenaar et al. (1997) used a basin

finding algorithm to estimate the areas of supergranular network cells. The application of this technique on the Ca-K images gave a cell size of about 15 Mm. A similar technique used by Srikanth et al. (2000) showed a cell size of 25 Mm, close to the most commonly known size of the network cells. Schrijver et al. (1997) used a gradient-based tessellation algorithm on the Ca-K images to find the network boundaries. This is a very effective technique to find the area of the network cells. The skeleton method (Berrilli et al. 1998), along with a cellular automaton method (Berrilli et al. 1999) applied to the Precision Solar Photometric Telescope (PSPT) Ca-K high pass filtered binary images, showed the area distribution of the network cells. From this method it is found that the network cells have a characteristic cell size of about 24 Mm.

The techniques to measure the plage and network areas, including the gradient-based tessellation algorithms (Schrijver et al. 1997), the image decomposition method (Harvey & White 1999; Worden et al. 1998) and skeletonizing iterative procedure (Ermolli et al. 2003), are restricted to small time intervals and do not include one complete solar cycle. However, many others (Tlatov et al. 2009) have tried to estimate the variation in the plage indices over several solar cycles using the digitized data sets of Kodaikanal, Mt. Wilson, etc. Though the overall pattern in the variation of the plage areas match well from each of the observatories, their magnitudes seem to be different for different observatory data sets (Ermolli et al. 2009).

From the measurements on a 2.4'' square aperture, Skumanich et al. (1975) showed that the average network has a brightness of 1.27 compared to that of the average non-network undisturbed chromosphere and covers 39% of the quiet Sun. They probably referred to the active network. Worden et al. (1998) analyzed 1400 Ca-K line spectroheliograms covering parts of solar cycle 21 and 22 with a spatial resolution of 8.5'' and defined the structures in Ca-K line spectroheliograms in four categories: plages, enhanced network, active network and quiet Sun. They systematically identified these components using different intensity thresholds and the minimum size for each category. The identified plages show intensity contrast relative to the quiet Sun greater than 2.776, and minimum values of 1.44. Similarly, the upper and lower level intensity contrasts are 2.06 and 1.37 for the enhanced network and 1.59 and 1.18 for the active network. They then built up the masks of the plages and found the plage area to be larger, by a factor of 2.8 compared to the plage areas published by the National Geophysical Data Center (NGDC).

Most of the time an enhanced or active network is present on the Ca-K line images and this makes it difficult to separate the network elements. Kodaikanal has been observing the full-disk images of the Sun since 1907. Recently, it has been updated with filter-based images and a charge coupled device (CCD) as an image acquisition system. The filter centered at 393.37 nm of the Ca-K wavelength has been used to image the Sun. The data obtained with this telescope provide a good opportunity to estimate the network element area index and its variation with time during the minimum solar activity period.

We applied a global fit method to the Ca-K data to normalize the images and used the threshold limits to automatically identify the network elements and plages on the solar surface. In this case, because of the extended solar minimum during the 2008–2010 period, we only have the quiet network features and a small amount of plages without the presence of the active and enhanced network. Hence, this is a good opportunity to study the network element area index.

In this paper, we give a brief description of the instrument used to obtain the Ca-K images at the Kodaikanal observatory and present the Ca-K network element area index variation results during the period between February 2008 and February 2011, spanning around three years.

In Section 2, we describe our instrument, which was used for obtaining the Ca-K data sets at the Kodaikanal observatory. The results on variation of the network element area index are presented in Section 3 and in Section 4 we discuss the various other studies and compare these studies with the results we obtained. We summarize the results in the final section.

2 INSTRUMENTS AND OBSERVATIONS

At the Kodaikanal observatory, photoheliograms of the Sun have been obtained on a daily basis since 1904 using a 15-cm aperture telescope, along with Ca-K spectroheliograms since 1907 and H_{α} spectroheliograms since 1912. Prior to this, the images of the Sun were recorded on specialized photographic emulsions. In 1995 we started using a narrow band filter at Kodaikanal, but still used the old siderostat and CCD camera with a $1K \times 1K$ format to take Ca-K filtergrams. We have now designed and fabricated a telescope to take Ca-K line and white light images of the Sun and named it the TWIN telescope. This telescope has been in operation since 2008 and has collected images during times with clear skies.

The TWIN telescope consists of two telescopes mounted on a single tracker. One of the telescopes takes the white light images in the continuum of the blue wavelength, and the other observes the Sun in the Ca-K wavelength. The focal length of the 150 mm objective lens from Zeiss is 2250 mm, and forms a 20.6 mm solar image. The optical system is capable of providing a spatial resolution of 0.7 arcsec at a wavelength of 400 nm. An interference filter with a 10 nm pass band centered at 395 nm is kept in front of the objective lens to avoid excess heat in the telescope, and also reduces the intensity to the required level to record the solar images. A thermally controlled narrow band interference filter centered at 393.37 nm with a passband of 0.12 nm is kept near the focus to isolate the central portion of the Ca-K line. The CCD camera with a $2K \times 2K$ pixel format with a 16-bit read out at 1 MHz records the Ca-K images. The image scale is $93''$ per mm, and so the pixel size with $13.5 \mu\text{m}$ provides a resolution of 1.25 arcsec per pixel. The images have been taken at a rate of one every 5 min. In case of activity on the Sun such as flares, we plan to obtain the images at an interval of 2 s by restricting the FOV and binning the CCD chip by 2×2 pixel.

The TWIN telescope has been functional since 2008 February 23 and can obtain the Ca-K line images of the Sun whenever the sky is clear. We have analyzed data up to 2011 February 28. The quality of the data is mostly homogeneous, except for a couple of gaps when the observations could not be made. The data obtained in cloudy conditions have not been used in this study. On a clear day we were able to get about 80 images, and in all we have used about 16 000 images in our study. We compute the average network element area for the day using all the images taken on that day, and the obtained data are dark subtracted and corrected for flat fielding.

3 RESULTS

A typical observed Ca-K image (Fig. 1) shows the network structure, a small plage region near the limb and the intensity gradient due to limb-darkening effects. No other types of large spatial scale intensity gradients are seen. When we started the solar observations with this telescope, the solar activity was in its declining phase. Hence, we do not see many active regions on the solar disk.

3.1 Network Cell Identification

In order to identify the network elements, we followed the procedure as given: (1) limb fitting to identify the image center and radius of the solar disk, (2) computing the limb-darkening profiles, (3) fitting a polynomial curve to the intensity profile and (4) using the thresholding method to identify the network cells and plages. The details of this method are described below.

3.1.1 Limb fitting method to identify the disk center and radius

In the technique to automatically detect features on the Sun, first it is essential to identify the center and radius of the Sun in terms of pixels. Hence, we computed the radius and center of the solar disk in the calibrated data sets. This was achieved by identifying the solar limb. The solar limb has a steep

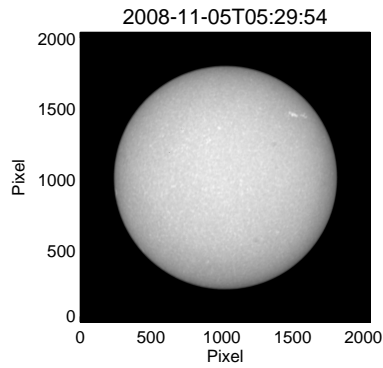


Fig. 1 Context image of Ca-K taken from the TWIN telescope, shown here for the observation date of 2008-November-05.

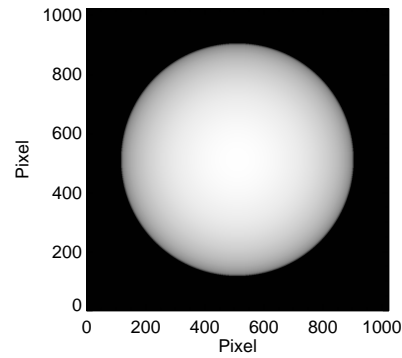


Fig. 2 Computed two-dimensional limb-darkening function used to remove the limb-darkening effect in the Ca-K image.

gradient between the solar disk and the surrounding region. We used the Sobel filter to detect the edge of the solar limb.

We then used a threshold value of five times the mean value of the Sobel filtered image to retain only the edges of the solar limb. We detected the eight points on the limb, four points on the east (E), west (W), north (N) and south (S) each, and the other four on the S-E, N-E, N-W and S-W points. Using the eight detected points on the solar limb, we applied a polynomial fitting to obtain the Sun's center and radius in terms of pixels. With this method we could identify the Sun's center and the solar limb with a one pixel accuracy.

3.1.2 Removal of limb-darkening

Intensity distribution is not uniform over the Sun's disk. It is large in the disk center and decreases towards the limb. In order to remove the non uniformity in the intensity due to the limb-darkening effect, we need to compute the limb-darkening profile. This has been achieved by the method described in Denker et al. (1999). These procedures have been adopted to remove the limb-darkening in the H_{α} images, and a similar procedure has been adopted here. We used the median value of intensity, which is less sensitive to asymmetric intensity distribution. To do this, the full-disk images are transformed to polar coordinates and at each radial position the median value is computed. This way gives the average radial profile and it is smoothed by large kernels. The final averaged and smoothed profile has been transformed to Cartesian coordinates. A resulting limb-darkening image is shown in Figure 2. We also show the profile of the limb-darkening corrected image in Figure 3 (left). This profile has been extracted for those pixels shown as dark lines in the middle of Figure 3 (right). The profile in Figure 3 (left) shows that in addition to the small amplitude due to small scale variations in the network, a small amount of residual gradient is present. We remove this gradient by fitting a polynomial as described in the next section. The limb-darkening function is computed for each image, and the correction is applied to the calibrated data set to remove the limb-darkening in the images.

3.1.3 Polynomial fitting and thresholding

The solar image in Ca-K displays several features such as network elements, an intra-network region and plages. Network cells have borders and they are more intense than the intra-network points. However, the network elements are less bright than the plage regions in the images taken in the

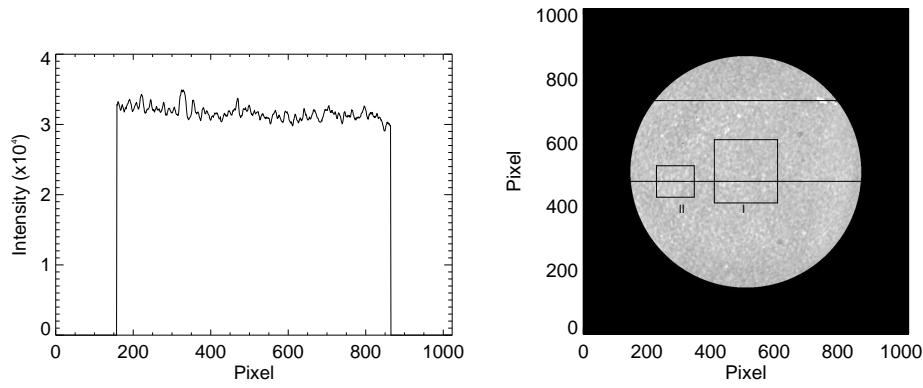


Fig. 3 *Left*: a typical intensity profile along a row of the image corrected for the limb-darkening effect. *Right*: the image obtained after limb darkening correction and polynomial fitting. The black boxes marked on the Ca-K image represent the regions for which the contours of the network elements are shown in subsequent figures. The black lines are the locations for which the profiles have been shown in Fig. 4.

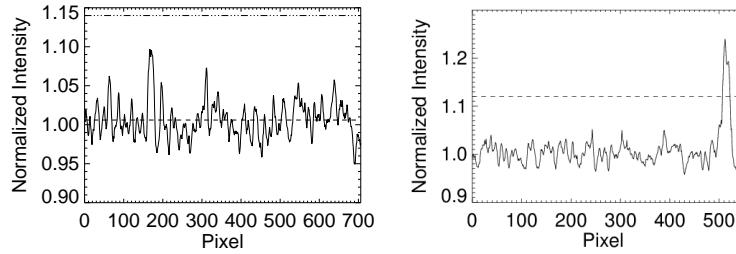


Fig. 4 Profile of row cuts (shown in Fig. 3 (*right*)) as two black lines). *Left*: the plot is shown for the quiet region. The horizontal dashed and dash-dot-dot lines in the plot indicate the intensity contrast levels of 1.006 and 1.12 respectively. *Right*: the plot is shown for the row cut that includes the plage region. The dashed line is drawn to show the intensity contrast level of 1.12.

Ca-K filters. We only used 90% of the inner solar disk in the network element/plage area index estimation as the fitted profile near the edges of the image leads to large uncertainty due to a sharp intensity gradient. Next, to segregate each of the features in the solar image we used the solar images after making the corrections for limb darkening as described above. Further, in order to remove the residual intensity gradient in the images, we repeatedly applied a third degree polynomial to one-dimensional (1D) row-wise and column-wise sliced pixels by keeping the mean level of the 1D data as before. By this method we make the background uniform and there are no variations in the background image. This procedure only keeps small-scale pixel to pixel intensity variations due only to the network elements and plages. The resulting image is shown in Figure 3 (*right*).

The background of the global fitted images has been normalized to a value equal to one. Figure 4 (*left*) shows the intensity distribution along a row with only the network and intra-network elements extracted from the line indicated by black in the middle of the image, as shown in Figure 3 (*right*). The dashed line and the dash-dot-dot line in the plot represent intensity contrast levels of 1.006 and 1.12, respectively. The pixels with a spatial scale of $2.5 \times 2.5 \text{ arcsec}^2$, with an intensity contrast less than 1.006, represent the background intra-network. The intensity contrast locations between 1.006

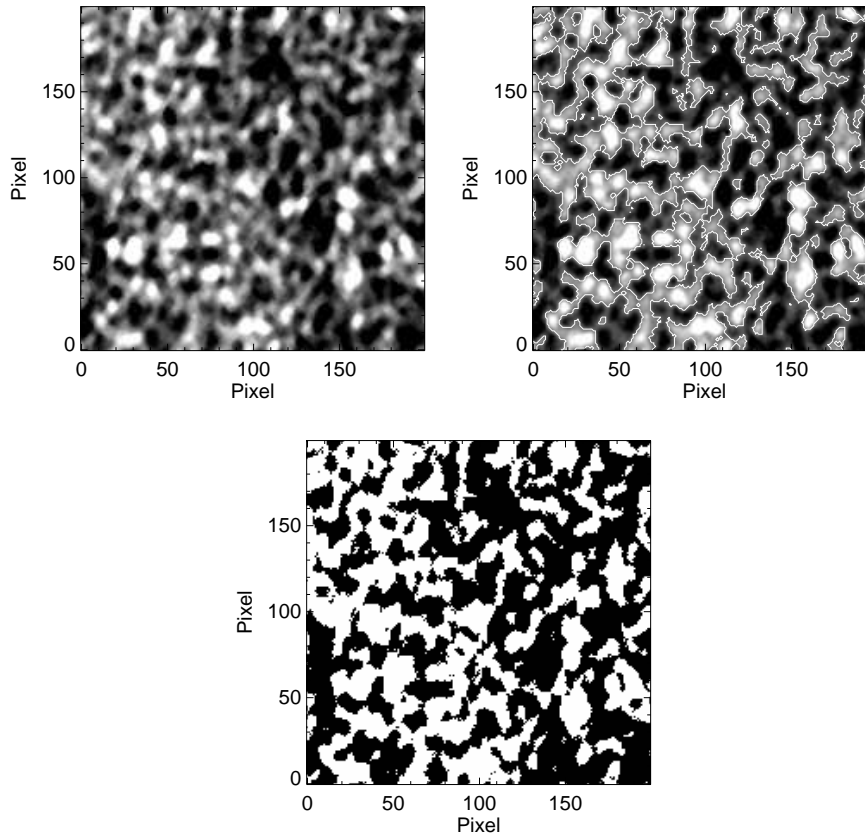


Fig. 5 *Top left*: a context image extracted from the center of the Sun's image (shown as region I in Fig. 3 (right)). *Top right*: a binary image of the left side image obtained using intensity contrasts of 1.006–1.12. *Bottom*: contours of the top right image overlaid onto the top-left image.

and 1.12 represent the network elements. Figure 4 (right) shows the intensity contrast distribution along a row extracted from a Ca-K image at a high latitude that has a small plage (this can be seen as a black line on the plage region in Fig. 3 (right)). The intensity contrast of the plage region is larger than 1.12.

In the following, we demonstrate that the selected threshold values of intensity contrast are able to segregate the network elements and Ca-K plage regions.

Figure 5 (top left) shows the image extracted from the central portion of the solar image (box number I in Fig. 3 (right)). The top right image is the binary image of the left-side image showing only the network elements extracted using upper and lower threshold values 1.006 and 1.12, respectively. A comparison of the left- and right-side images indicates that all the network elements lie in this contrast range. The bottom image shows the contours of the top-right image overlaid onto the top-left image. These maps show that once the background has become uniform, a fixed upper and lower threshold is able to separate the different network elements from each other.

Figure 6 shows the contours of the detected network elements overlaid onto the region II shown in Figure 3 (right). This map clearly shows that the contours coincide with the network elements, suggesting that the method is able to identify the network element features even near the limb.

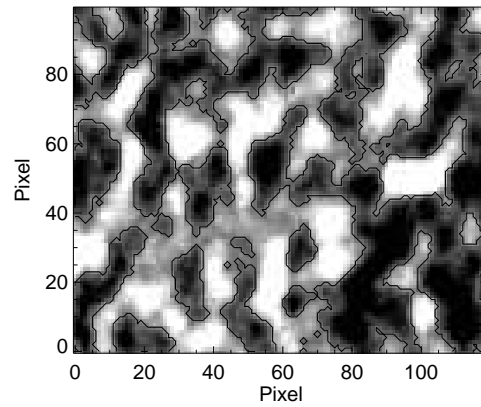


Fig. 6 Contours of the region obtained from the intensity contrast threshold values of 1.006 (lower) and 1.12 (upper) overlaid onto the region II shown in Fig. 3 (*right*).

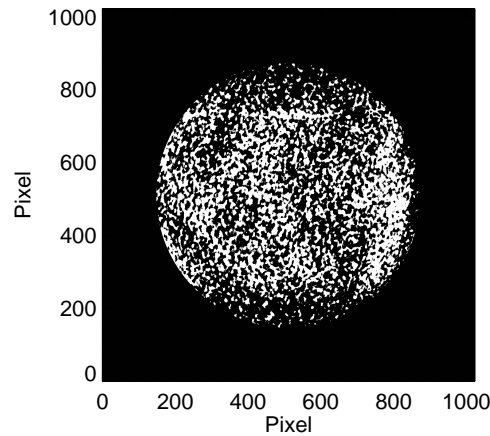


Fig. 7 Binary image for the extracted network elements using the upper and lower threshold values for the whole disk.

Figure 7 shows the extracted network elements on the whole disk. The extracted network pattern is uniform over the disk, except for some of the gaps that are seen in the polar regions which may be due to poor intensity contrast.

Once the network elements have been identified by the algorithm based on the threshold values of intensity contrast, it becomes a simple task to extract the plage region. In the absence of enhanced and active network elements during this period, we identified plage regions with an intensity contrast greater than 1.12. To make sure that this threshold value identifies only the plage region, the contours of the threshold region obtained from the algorithm are overlaid onto the Sun's image, as shown in Figure 8 (top left). Three different regions are magnified and the contours overlaid onto it. This is shown in Figure 8 (top right, bottom left and right). The contours shown in Figure 8 demarcate the plagues from the other regions. From this segregation of the individual regions it is now easy to estimate the network element area and plage area index.

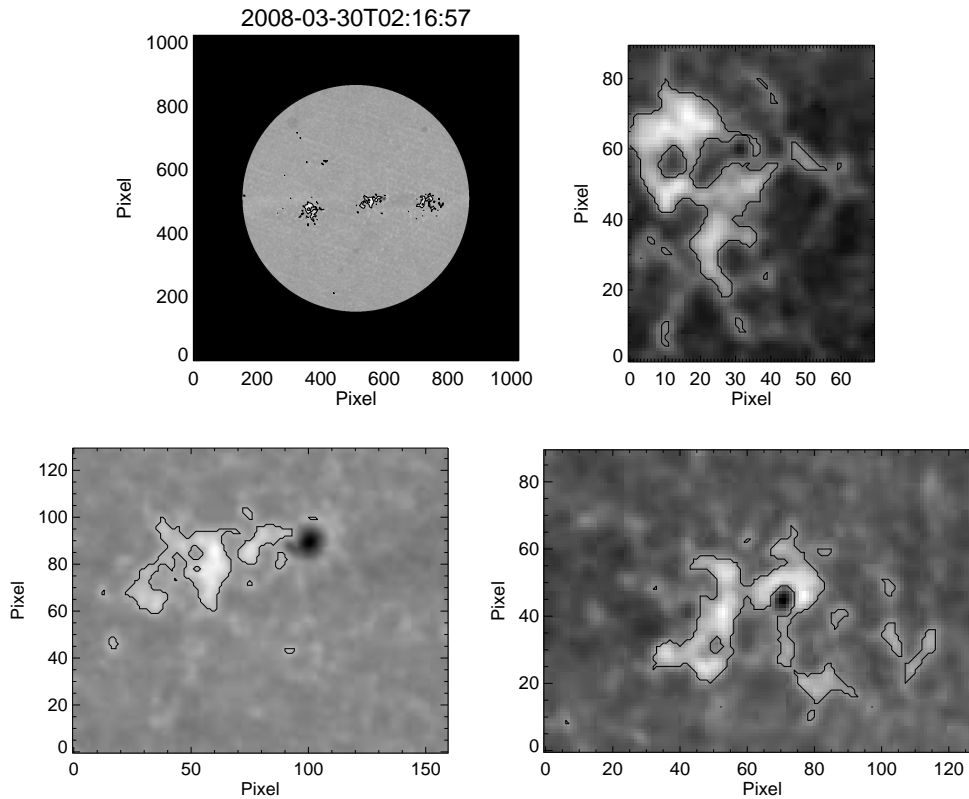


Fig. 8 *Top left*: the contours of the plage region detected by the algorithm overlaid onto the full-disk image and the contours of the detected plage regions overlaid onto the magnified portion of the first (*top right*), second (*bottom left*) and third (*bottom right*) plage regions seen in the full-disk image from left to right.

3.2 Network Element Area and Plage Area Index

The network element area index is expressed as a ratio of the area of the network elements occupied on the Sun to the area of the visible solar disk excluding the plage areas. We excluded the plage area from the visible solar disk area while computing the network element index to study absolute variations of the index in this period by making the data uniform. We estimated the network element area index for 90% of the solar disk. The remaining 10% close to the limb is simply discarded as a large projection effect. It is difficult to extract the remaining network elements because of improper limb-darkening correction at the edges. We computed the radius of the Sun for a particular epoch. The area occupied by all the pixels in the contrast range from 1.006 to 1.12 was taken into consideration for the network element area index calculation and the resulting network element area index is converted into a percentage using the 90% value of the visible area of the solar disk.

In order to study the variations in network element area index over the years, we plotted the daily average value of the network element area index of the observations for the period from February 2008 to February 2011 (Fig. 9). The plot shows that the network element occupies about 32% of the solar disk from February 2008 until August 2008. Then the network element area decreases monotonically until February 2009. After that it remains flat, with some small undulations in its value. The error in measuring the network element area is 2% of the daily average network element

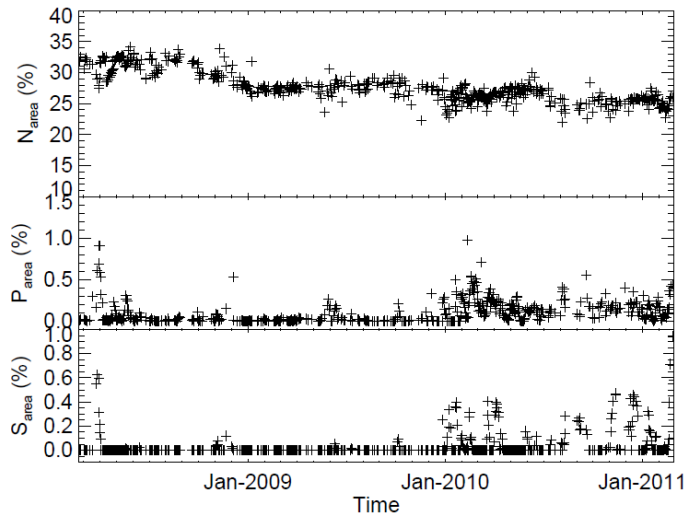


Fig. 9 *Top*: the daily average value of the network element area index (N_{area}), *middle*: the plage area index (P_{area}) and *bottom*: the sunspot area index (S_{area}) expressed in terms of percentage, plotted over a period from February 2008 to February 2011.

area index, and the error was estimated by varying the lower threshold value. The upper threshold value is kept at 1.12, as it is a large value and it did not affect our result by more than 0.02%. The network element area decreased by about 7% from February 2008 to 2011. The plage area during the solar minimum period and the ascending phase of solar cycle 24 occupies less than 1% of the solar disk. It should be noted here that the area occupied by the network element over the solar disk is not corrected for the projection effect. The network elements cover the disk almost uniformly. We are looking for variations in the network element area index with time. Although the values of the network element area are equally affected by the projection effect over the observing period, the percentage of the area may only change marginally as the network element area changes proportionally to the visible area of the solar disk after the foreshortening correction. Thus, the observed differences in the area index over the three years (7%) appear real and may not be due to the foreshortening effect. We may consider this for the study of long-term variations of the network element area index in the future. The sunspot area index is also shown at the bottom of Figure 9 for comparison. Similar to the plage area index, the sunspot area also covered less than 1% of the solar disk during the extended minimum period.

4 DISCUSSION

By using Ca-K images obtained from the TWIN telescope at the Kodaikanal observatory, and by applying a novel technique, we were able to separate the network elements from other structures such as background and plage regions. After applying this technique, the contrast between the network elements is almost the same at all disk positions, and hence we were able to identify the network elements by using single upper and lower threshold values. From the identified network elements we computed the network element area index over the minimum period of the solar cycle until the ascending phase of solar cycle 24.

It is not a straight forward process to compare our results with those obtained by others in the past. This is mainly because of the different pass bands of the filters used in previous observations

and the different spatial resolutions and seeing effects of the instruments. All these parameters affect the contrast of the network element features. Many of them have measured the network area for a few days and some of them have measured it for a few years, and also included enhanced and active networks, whereas our study only deals with quiet network elements. Singh & Bappu (1981) reported that the Ca-K network size is smaller in the quiet region during the maximum phase of the solar cycle compared to that during the minimum period. Worden et al. (1998) measured the intensity contrasts of the various features observed in Ca-K images and found that the intensity contrast of the plages and enhanced network regions do not change over the solar cycle, though their numbers will go down during the solar minimum. They estimated that the plage and enhanced network cover the solar surface by 13% and 10%, respectively, during the solar maximum. By using the Ca-K images from the Rome PSPT, Ermolli et al. (2003) estimated that the network coverage over the disk changes by 6% over the ascending phase of solar cycle 23, being small during the minimum and increasing up to the solar maximum. Walton et al. (2003), using the San Fernando observatory Ca-K images, found that the area covered by the active region reduces by a factor of ~ 20 from maximum to minimum. On the other hand, the area covered by the small regions (including the network) reduces by a factor of about two from maximum to minimum of the activity cycle. Hagenaar et al. (2003) observed that the different magnetic flux concentrations in the network elements behave differently during different phases of the solar cycle. Meunier (2003) reported that the magnetic flux in the network elements are in phase with the solar cycle. Jin et al. (2011) obtained a result similar to Hagenaar et al. (2003), and also reported that the fractional area of the quiet regions is anticorrelated with the solar cycle, but that their total magnetic flux is correlated with the solar cycle. McIntosh et al. (2011) found that the mean supergranulation length scale changes from solar maximum to minimum. They also found that there is a difference of about 0.5 Mm in the mean radius of the supergranulation during the current solar minimum compared to the previous solar minimum. All these analyses focus mostly on the contrast of the network or the area of the network, and some of them use magnetograms to measure the variations of the quiet Sun flux with the solar cycle. In our study, we concentrated on the area occupied by the network elements over the solar disk during the minimum period and the ascending phase of solar cycle 24. We found a decrease of about 7% in the disk coverage of the network element from the minimum phase to the ascending phase of solar cycle 24. During the prolonged minimum period of solar cycle 23, there are a few or no active regions observed on the Sun. One of the main concepts of network field generation is the decay of the active regions. Since the number of active regions reduces to a few or none, the magnetic fields of the network may also have been reduced and hence the area occupied by the network elements was also reduced. It could also be possible that we are observing the anticorrelated component of the quiet Sun network here (Jin et al. 2011). Long-term network element data analysis is required to confirm this conjuncture.

5 SUMMARY

The Kodaikanal observatory has provided 100 years' worth of data with Ca-K and white light images. To continue the availability of data for future solar cycles, we have developed a CCD-based imaging system at Kodaikanal. The advantage of this system compared to the previous one is that it can take a burst of images within a few hours. We have described a method to determine the network element area and plage area index separately. We applied this technique to the data obtained from the new telescope at Kodaikanal, and using this technique it was easy to separate the network and plage regions in the limb-darkening corrected images. The results obtained from this technique indicate that the network elements occupy about 30% of the solar disk. However, the network element area index slowly decreases by about 7% during a period of about three years. The decrease in the daily average of the network element area index over a period of three years could be related to the extended minima and continuing low activity phase. We need a longer time sequence of data to

understand this variation in the network element area index and we plan to use digitized data for this study.

Acknowledgements We would like to thank the anonymous referee for his/her constructive comments on this paper. Jagdev Singh is grateful to F. Gabriel and his team for designing, fabricating and installing the telescope at Kodaikanal. We thank Mr. Anbazhagan and K. Ravi for developing the guiding system for the telescope. J. S. acknowledges the help of S. Muneer in the initial stages of the project and thanks F. George, S. Ramamoorthy, P. Loganathan, P. Michael, P. Devendran, G. Hariharan, K. Fathima and S. Kamesh for their help in executing different parts of the project.

References

- Berrilli, F., Ermolli, I., Florio, A., & Pietropaolo, E. 1999, *A&A*, 344, 965
Berrilli, F., Florio, A., & Ermolli, I. 1998, *Sol. Phys.*, 180, 29
Denker, C., Johannesson, A., Marquette, W., et al. 1999, *Sol. Phys.*, 184, 87
Ermolli, I., Berrilli, F., & Florio, A. 2003, *A&A*, 412, 857
Ermolli, I., Solanki, S. K., Tlatov, A. G., et al. 2009, *ApJ*, 698, 1000
Foukal, P., Bertello, L., Livingston, W. C., et al. 2009, *Sol. Phys.*, 255, 229
Hagenaar, H. J., Schrijver, C. J., & Title, A. M. 1997, *ApJ*, 481, 988
Hagenaar, H. J., Schrijver, C. J., & Title, A. M. 2003, *ApJ*, 584, 1107
Harvey, K. L., & White, O. R. 1999, *ApJ*, 515, 812
Jin, C. L., Wang, J. X., Song, Q., & Zhao, H. 2011, *ApJ*, 731, 37
McIntosh, S. W., Leamon, R. J., Hock, R. A., Rast, M. P., & Ulrich, R. K. 2011, *ApJ*, 730, L3
Meunier, N. 2003, *A&A*, 405, 1107
Schrijver, C. J., Hagenaar, H. J., & Title, A. M. 1997, *ApJ*, 475, 328
Singh, J., & Bappu, M. K. V. 1981, *Sol. Phys.*, 71, 161
Skumanich, A., Smythe, C., & Frazier, E. N. 1975, *ApJ*, 200, 747
Srikanth, R., Singh, J., & Raju, K. P. 2000, *ApJ*, 534, 1008
Tlatov, A. G., Pevtsov, A. A., & Singh, J. 2009, *Sol. Phys.*, 255, 239
Walton, S. R., Preminger, D. G., & Chapman, G. A. 2003, *ApJ*, 590, 1088
Worden, J. R., White, O. R., & Woods, T. N. 1998, *ApJ*, 496, 998